

12 Mar 1991, 2:30 pm - 3:30 pm

## BEM-FEM Hybrid Analysis for Topographical Site Response Characteristics

Hirokazu Takemiya  
*Okayama University, Okayama, Japan*

Masaki Ono  
*Hazama-Gumi, Ltd., Tokyo, Japan*

Kiyotaka Suda  
*Hazama-Gumi, Ltd., Tokyo, Japan*

Follow this and additional works at: <https://scholarsmine.mst.edu/icrageesd>



Part of the [Geotechnical Engineering Commons](#)

### Recommended Citation

Takemiya, Hirokazu; Ono, Masaki; and Suda, Kiyotaka, "BEM-FEM Hybrid Analysis for Topographical Site Response Characteristics" (1991). *International Conferences on Recent Advances in Geotechnical Earthquake Engineering and Soil Dynamics*. 5.

<https://scholarsmine.mst.edu/icrageesd/02icrageesd/session08/5>



This work is licensed under a [Creative Commons Attribution-Noncommercial-No Derivative Works 4.0 License](#).

This Article - Conference proceedings is brought to you for free and open access by Scholars' Mine. It has been accepted for inclusion in International Conferences on Recent Advances in Geotechnical Earthquake Engineering and Soil Dynamics by an authorized administrator of Scholars' Mine. This work is protected by U. S. Copyright Law. Unauthorized use including reproduction for redistribution requires the permission of the copyright holder. For more information, please contact [scholarsmine@mst.edu](mailto:scholarsmine@mst.edu).



# BEM-FEM Hybrid Analysis for Topographical Site Response Characteristics

Hirokazu Takemiya, Professor, Department of Civil Engineering, Okayama University, Okayama, Japan  
 Masaki Ono, Hazama-Gumi, Ltd., Tokyo, Japan  
 Kiyotaka Suda, Hazama-Gumi, Ltd., Tokyo, Japan

**SYNOPSIS:** This paper concerns an amplification of seismic ground motions by a certainly shaped surface soil deposits in view of its topographical configuration. Different hybrid methods of the boundary element method (BEM) and the finite element method (FEM) are used for the two-dimensional (2-D) analysis. In the analysis, the far field impedance is first evaluated by BEM then it is incorporated into the near field FEM analysis based on the weighted residual method. The steady state responses for different types of harmonic incident waves are investigated. Some useful findings are pointed out in comparison with the one-dimensional (1-D) results.

## INTRODUCTION

Observations from past earthquake damages are very indicative of the surface soft soil amplification for the seismic waves from the rock-like base level. The vertical shear wave propagation or the 1-D theory, for instance the computer code SHAKE (Shnoble et al., 1972) has been dominantly employed for evaluating such surface soil amplification. However, in view of the surface/subsurface irregularities such as a canyon or an alluvial valley, the 2-D modeling should be made. Such analysis started on the antiplane motion for its simplicity; the analytic solution by Trifunac (1973), Wong and Trifunac (1974); the discrete wave number solution by Aki and Larner (1970), and Campillo and Bouchon(1985); the direct boundary element method (DBEM) by Wong and Jennings (1975), the indirect boundary element method (IDBEM) or source potential method by Sanchez-Sesma and Esquivel (1979), Dravinski (1982), Shinozaki (1988); and the hybrid method between the BEM for the far field and the finite element method (FEM) for the near field by Toki and Sato (1983). These literatures pointed out the significance of the surface / subsurface effect on the wave scattering through the frequency domain analysis. The investigation for inplane motion was then addressed by DBEM by Kobayashi (1983), and Abascal and Dominguez (1984); by IDBEM by Wong (1982), Dravinski and Mossessian (1987), Vogt et al. (1988); and recently by the hybrid method of FEM and IDBEM by Mossessian and Dravinski (1987), Khair, Datta and Shah (1989). Introducing source potentials to interpret scattered wave field, which takes account of the semi-infinity condition of a halfplane automatically, is an effective solution method but some due care should be taken for the source position and its numbers. The author's recent paper (Takemiya and Arioka, 1990; Takemiya et al., 1990) gives information about these.

In the companion paper (Takemiya et al., 1990), the wave scattering analysis due to topographical boundary condition is executed for a harmonic steady state. Besides the DBEM, the so-called hybrid procedure of the BEM for far field and the FEM for near field of irregular surface soil deposits is developed based on the weighted residual concept to make use of the advantages of the respective method in the modeling. The substructure approach is taken in the computation process; first the far field impedance function is computed and then incorporated for the FEM near field analysis. Different formulations are employed; one is the DBEM application along the interface between near and far fields, the other is the application of the IDBEM which takes certain offset sources as intermediate unknown parameters.

Herein, the point of investigation is addressed to interpreting the effect of 2-D site topography with regard to incident wave types and wave length and to clarifying the situation where the

1-D analysis can be applied to compute the soil amplification. The trapezoidal-shape soil deposits, as illustrated in Fig.1, is considered at some representative non-dimensional frequencies as defined by the ratio  $\eta$  of the surface width of soil deposit  $2A$  to the incident wave length, i.e.  $\eta = 2A/\lambda$ . The comparative studies are made for the different Green functions to be used; i.e., the solutions for concentrated /distributed source forces for a uniform /layered halfplane in addition to the Stokes' solution for a full space. For seismic analysis, different types of incident inplane waves such as SV, P and Rayleigh waves are assumed. Special attention has been paid to the soil layering with regard to the aspect ratio  $B/D$  of soil deposit width  $B$  to its depth  $D$  to see the difference of 2-D response from that of 1-D analysis for the frequency range of seismic viewpoint. The numerical results for the surface displacement are very indicative of the topographical configuration of the soil deposits for incident waves under certain situation.

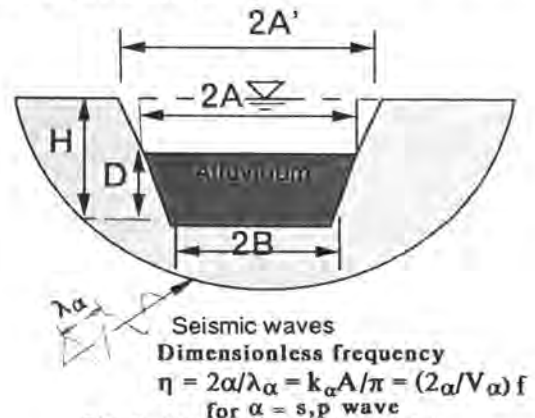


Fig. 1 Topographical site model

## SUBSTRUCTUE FORMULATION

### Superposition of wave fields

The soil domain to be analyzed is substructured into the surface soil deposits and the surrounding far field. The input seismic motion is prescribed as an incident wave to be defined at the far field (denoted by superscript  $f$ ). The presence of the surface soil deposits with subsurface topography, reflecting the incident waves at the interface with the far field, generates scattered waves (denoted by the superscript  $s$ ) in the far field. The near field is composed of the transmitted waves and the reflected waves from the free surface and the total wave field is defined as refracted wave field. See Fig.2. Thus, the displacement and traction representation becomes as

$$u = u^f + u^s \quad t = t^f + t^s \quad (1),(2)$$

The scattered wave propagation of the far field, presumably comprising uniform or uniformly layered soils, is modeled by the BEM either by the direct method or by the indirect method with source force application. The near field, on the other hand, comprising nonhomogeneous soils and normally includes structures, is modeled by the FEM. The weighted residual technique is used to advantage to formulate the coupling between these FEM and BEM domains.

**BEM for exterior domain**

(i) Direct BEM

Based on the Somigliano equation, we get the following boundary integral equation for the scattered wave field in the exterior domain.

$$cu(x) + \int_{S_b} G_t(x,y)u^s(y)ds(y) = \int_{S_b} G_u(x,y)t^s(y)ds(y) \quad (3)$$

in which  $G_u$  and  $G_t$  are the Green functions for displacement and traction, and  $u_b$  and  $t_b$  are the unknown displacement and traction on the interface  $S_b$  and  $c$  is the so-called free term. The discretization of Eq.(3) with the interpolation function,  $N_u$  and  $N_t$

$$\begin{aligned} u_b^f(y) &= N_u(y) \hat{u}_b^f, \quad t_b^f(y) = N_t(y) \hat{t}_b^f \\ u_b(y) &= N_u(y) \hat{u}_b, \quad t_b(y) = N_t(y) \hat{t}_b \end{aligned} \quad (4),(5),(6),(7)$$

can be expressed as

$$H \hat{u}_b^s = G \hat{t}_b^s \quad (8)$$

or in terms of the total wave field

$$H(\hat{u} - \hat{u}^f) = G(\hat{t} - \hat{t}^f) \quad (9)$$

in which  $G$  and  $H$  are computed elementwise from the integral of the product of  $G_u$  and  $N_u$ , and  $G_t$  and  $N_t$ , respectively. For singular elements, the subelement technique is used for the Cauchy principal integration. The diagonal terms of  $H$  are computed from the static rigid body condition. Care should be taken for the infinite domain with inclusion of an elastic domain in contrast to the one with a cavity inside. If the Stokes solution is used for the kernel function in Eq.(3), additional nodes should be placed on the far field surface (denoted by subscript  $f$ ). The latter nodes which makes the free field are differentiated from the interface nodes (by subscript  $b$ ) so that

$$\begin{bmatrix} H_{bb} & H_{bf} \\ H_{fb} & H_{ff} \end{bmatrix} \begin{bmatrix} \hat{u}_b \\ \hat{u}_f \end{bmatrix} = \begin{bmatrix} G_{bb} & G_{bf} \\ G_{fb} & G_{ff} \end{bmatrix} \begin{bmatrix} \hat{t}_b \\ \hat{t}_f \end{bmatrix} = \begin{bmatrix} H_{bb} & H_{bf} \\ H_{fb} & H_{ff} \end{bmatrix} \begin{bmatrix} \hat{u}_b^f \\ \hat{u}_f^f \end{bmatrix} - \begin{bmatrix} G_{bb} & G_{bf} \\ G_{fb} & G_{ff} \end{bmatrix} \begin{bmatrix} \hat{t}_b^f \\ \hat{t}_f^f \end{bmatrix} \quad (10)$$

Condensing out the free field nodes "b" and leaving the interface nodes "f" only yield the traction at the interface  $S$  as

$$\hat{t}_b = (G_{bb})^{-1} H_{bb} \hat{u}_b - (G_{bb})^{-1} H_{bb} \hat{u}_b^f - \hat{t}_b^f \quad (11)$$

with

$$G_b = G_{bb} - H_{fb} (H_{ff})^{-1} G_{fb} \quad H_b = H_{bb} - H_{bf} (H_{ff})^{-1} H_{fb} \quad (12),(13)$$

If the halfplane Green function is used, no need to place the free surface nodes  $F$  for the far field, so that

$$\hat{t}_b = (G_{bb})^{-1} H_{bb} \hat{u}_b - (G_{bb})^{-1} H_{bb} \hat{u}_b^f - \hat{t}_b^f \quad (14)$$

(ii) Indirect BEM (Source force method)

We assume that the scattered wave field will be reproduced by imposing appropriately distributed fictitious force  $p(x)$  on a surface  $S'$  ( $S'$  would be located on the interface  $S$  but may be

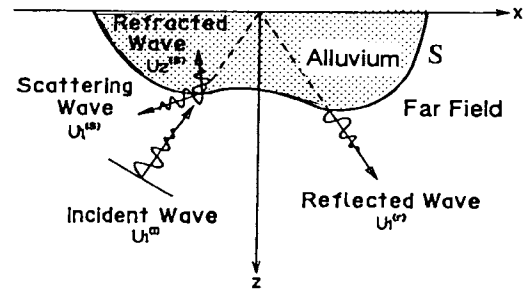


Fig.2 Wave scattering by alluvium deposit

offset by a small distance  $\epsilon$  from it from the computations reason) in the free field. The relevant Green functions for displacement  $G_u(y,x)$  and traction  $G_t(y,x)$  for point / uniform distributed forces are referred to the authors paper (Takemiya and Arioka, 1990.a, b) Then, the displacement  $u_p$  and traction  $t_p$  at any position  $y$  are evaluated as

$$u_p^s(y) = \int_{S'} G_u(y,x) p(x) ds(x) \quad t_p^s(y) = \int_{S'} G_t(y,x) p(x) ds(x) \quad (15),(16)$$

The unknown forcing function  $p(x)$  will be determined from the weighted residuals equations as stated below.

**FEM for interior domain**

The FEM formulation starts with the virtual work equation in the concerned domain.

$$\int_V \delta \epsilon^T \sigma dv = \int_V \delta u^T (-\rho \omega^2) u dv + \int_S \delta u^T p ds \quad (17)$$

in which  $s$  = stress,  $\epsilon$  = strain,  $u$  = displacement,  $\rho$  = density,  $\delta(\ )$  mean the virtual quantities. After discretization we get the governing equation as

$$\begin{bmatrix} D_{ii}^n & D_{ib}^n \\ D_{bi}^n & D_{bb}^n \end{bmatrix} \begin{bmatrix} \hat{u}_i^n \\ \hat{u}_b^n \end{bmatrix} = \begin{bmatrix} 0 \\ N^T t_b^n ds \end{bmatrix} \quad (18)$$

in which  $D$ 's defining the dynamic stiffness matrices

$$D^n = -\omega^2 M^n + i \omega C^n + K^n \quad (19)$$

with  $M^n$ ,  $C^n$  and  $K^n$  denoting, respectively the mass, damping and stiffness matrices, all of which are derived from the standard procedure, and  $i$  = imaginary unit.

**Hybrid approach**

The governing equation of the coupled system for the above BEM and FEM domains is made such that the degrees of freedom (DOFs) of the FEM are maintained and the far field impedance function derived from the BEM analysis, which is compatible with the DOFs of the interface boundary, is substituted in the former equation. The weighted residual equations for displacement and traction are used for this purpose.

$$\int_S w_d^T(y) (u_{b,BEM} - u_{b,FEM}) ds(y) = 0 \quad (20)$$

$$\int_S w_t^T(y) (t_{b,BEM} + t_{b,FEM}) ds(y) = 0 \quad (21)$$

in which  $w_d(y)$  and  $w_t(y)$ , defining the independent weighting functions, respectively, for displacement and traction, are adopted as follows:

$$w_d(y) = t_p^s(y) \quad \text{and} \quad w_t(y) = u_b(y) \quad (22),(23)$$

i) For the direct BEM approach, Eq.(20) is automatically satisfied so that Eq.(21) only is claimed. This converts the action into the FEM nodal forces.

$$L(t_b^f + t_b^s) = P_b^n \quad (24)$$

where which L denotes the transformation matrix of the impedance matrix for the far field is then defined as

$$K_{bb}^* = L G^{-1} H \quad (25)$$

Hence, the total governing equation is obtained.

$$\begin{bmatrix} D_{ii}^n & D_{ib}^n \\ D_{bi}^n & D_{bb}^n + K_{bb}^* \end{bmatrix} \begin{Bmatrix} \hat{u}_i^n \\ \hat{u}_b^n \end{Bmatrix} = \begin{Bmatrix} 0 \\ K_{bb}^* \hat{u}_b^f - L t_b^f \end{Bmatrix} \quad (26)$$

ii) For the indirect BEM approach, after discretization, Eqs.(20) and (21) result in

$$G^T P + H(u_b^f - \hat{u}_b) = 0 \quad H^T P + P_b^f + P_b^n = 0 \quad (27), (28)$$

The matrices G and H are properly defined when Eqs.(22) and (23) are substituted and computed elementwise. Eliminating the unknown force intensities P from Eqs.(27) and (28) derives the far field impedance  $K_{bb}^*$  and the effective input forces  $P_b^f$  to the FEM domain. Hence, the total governing equation results.

$$\begin{bmatrix} D_{ii}^n & D_{ib}^n \\ D_{bi}^n & D_{bb}^n + K_{bb}^* \end{bmatrix} \begin{Bmatrix} \hat{u}_i^n \\ \hat{u}_b^n \end{Bmatrix} = \begin{Bmatrix} \hat{P}_i^n \\ K_{bb}^* \hat{u}_b^f - \hat{P}_b^f \end{Bmatrix} \quad (29)$$

with

$$K_{bb}^* = H^T (G^T)^{-1} H \quad (30)$$

## NUMERICAL ANALYSIS AND DISCUSSION

The validation of the present hybrid method is made by comparing the results with the available ones for a half-circular soil deposit and a canyon for different types of incident waves (Dravinski and Mossessian, 1987; Wong, 1982; Takemiya and Arioka, 1990). After confirming the accuracy, the parametric study is conducted for the trapezoidal shaped layered soil deposits on a uniform halfplane base. The dimensions and the soil properties are described in Figs.3 and Table 1. The models of different aspect ratios  $B/D = 1.3$  and  $2.7$  are investigated. The types of the incident waves considered are the P, SV body waves of various angle of incidence, and the Rayleigh surface wave. The main parameter in focussing our attention to the deposit's behavior is the dimensionless frequency  $\eta = 2A/\lambda_{sv} = (2A/V_s)f$  or  $\eta = 2A/\lambda_p = (2A/V_p)f$  in which  $2A$  is the surface width of soil deposit,  $\lambda_{sv}$  is the S-wave length,  $\lambda_p$  is the P-wave length for the far field halfplane and  $f$  is the frequency concerned.

For the DBEM the Stokes solution for a full space is adopted so that a certain number of additional nodes must be placed on the far field surface adjacent to the near field in order to make a free surface (see Fig. 3.a). In the IDBEM, the Green function of the Lamb type solution for a layered halfplane due to a uniformly distributed source force is effectively employed (Takemiya, et al., 1990; Takemiya and Arioka, 1990a, 1990b). These sources are offset from the actual boundary by around 1/6 of the wave length concerned (see also Fig.3.b). Note that the FEM modeling is taken to cover a neighboring portion of the far field as a transit area from near field to far field. This treatment works for improving the solution accuracy when the soil stiffness changes drastically from near to far fields. Linear isoparametric

elements are used in discretizing both the BEM and FEM domains.

The 1-D model is first considered to get a general crude insight about the behavior the soil deposits and the resulting surface resonance curve is depicted in Fig.4. In view of the fundamental frequency  $f_1$ , the value of  $\eta$  is assumed as from 0.25 through 3 for the 2-D analysis. The latter results are shown in Figs. 5 through 7 for the Case 1 in which the surface response of the soil deposits is presented in a normalized form by the far field surface response (the scale at the left hand side) and by the surface response of the horizontally layered soils without topographical consideration (the scale at the right hand side). Note that the computation accuracy among the methods is quite well for frequency range up to  $\eta=3$  for SV wave and Rayleigh wave incidence and up to  $\eta=2$  for P wave incidence. This may be interpreted from the fact that the actual frequency  $\omega=2\pi f$  for P wave is about two times larger than that for SV wave when the nondimensional frequency  $\eta$  is kept to a constant value. If the more deliberate source numbers and their location are taken, the better matching between IDBEM and DBEM will be expected. However, as far as our attention is focussed to extended structures on soft soil deposit, the value of  $\eta$  may be confined as, say  $\eta < 2$ .

From the topographical site analysis for  $D/H=1$  (Figs.5 though 7), it is clear that the surface response is significantly characterized by the type of incident waves and by the angle of their incidence. The effect of the dimensionless frequency is also remarkable. For vertical SV wave incidence at low dimensionless frequency, the response mode with only one peak results at the center of soil deposits surface which is about two times greater response than the far field surface response, while at high dimensionless frequency the response mode with multiple peaks appears, giving the greater values at the ends of soil deposits surface than the far field surface response. The vertical response component is generated significantly as the frequency grows, say  $\eta > 1$  at the surface over oblique base. The effect of incident angle increases also the response at the surface over the oblique base; at  $\eta=1$  more than two times greater value of the far field response results. The same tendency can be observed for P wave incidence with reversing the horizontal and vertical components. The Rayleigh wave incidence yield different amplification than the oblique SV wave incidence, although both have a propagation effect in horizontal direction. Therefore, the response for a Rayleigh wave may not be replaced by an oblique SV wave incidence.

In order to see the topographical effect on the behavior of soil deposits, the comparison is made between the 2-D and 1-D analyses. Figs. 8 and 9 show the vertical response profiles for the aspect ratio  $B/D = 1.3, 2.7$ , respectively. We note that for the soil deposit of small aspect ratio  $B/D = 1.3$ , the presence of the oblique subsurface leads the more deviated response profiles than the 1-D solution except at very low frequency due to the wave scattering, while the case for the aspect ratio  $B/D = 2.7$  gives rise to the almost same response profile with the 1-D amplification in the low to intermediate frequency range. We may state that for the portion of layer longer than the distance  $B/D > 3$  the 1-D analysis may valid around the predominant surface layer frequency  $f_1$  from the 1-D analysis. And the subsurface topography tends to increase the surface response over the flat base in the higher frequency range above  $f_1$  while decreases it below  $f_1$ .

Figs.10 indicates the effect of the soil deposits depth on the surface amplification for the Case 1 with D/H as a parameter. Clear difference is observed according to this value. The fact that the highest peak is attained by different topography at different frequency may be interpreted by the resonance of the surface alluvium deposit, and also the drastic change of the response mode for D/H = 1.0 from  $\eta = 0.5$  to 1.0.

### CONCLUSION

The advantage of the hybrid method between BEM and FEM is noted for the seismic analysis of topographically certain-shaped overlying soil deposits on a halfplane base. Indirect and direct BEM approaches give an excellent matching for the surface response evaluation in the dimensionless frequency (wave length v.s.soil deposit surface width) important for the analysis of extended civil engineering structures. From the parametric study, the site topographical effect, which is indicated as the difference from the far field response and also from the 1-D response analysis of the concerned soil deposits, is clarified with respect to the incident wave type and its angle of incidence and to its dimensionless frequency.

### REFERENCES

Abascal,R. and Dominguez,J., Dynamic Behavior of Strip Footings on Non-homogeneous Viscoelastic Soils, Int. Symp. Dynamic Soil-Struct. Int. Minneapolis, Balkema, 1984.

Aki,E. and Larner,K.L., Surface Motion of a Layered Medium Having an Irregular Interface Due to Incident Plane SH Waves, J. Geophysical Research, Vol.75, No.5,1970, pp.933-954.

Campillo,M. and Bouchon,M., Synthetic SH Seismograms in a Laterally varying Medium by Discrete Wavenumber Method, Geopys. J.R. Astr. Soc., Vol.83, 1985, pp.307-317.

Dravinski, M., Scattering of SH Waves by Subsurface Topography, J. Eng. Mech. Div., ASCE, Vol.108, No.EM1, 1982, pp.1-7.

Dravinski,M. and Mossessian, T.K., Scattering of Plane Harmonic P,SV, and Rayleigh Waves by Dipping Layers of Arbitrary Shape, Bull. Seism. Soc. Amer., Vol.77, No.1, 1987, pp.212-235.

Khair, K.R., Datta,S.K. and Shah, A.H., Amplification of Obliquely Incident Seismic Waves by Cylindrical Alluvial Valleys of Arbitrary Cross-sectional Shape. Part I. Incident P and SV Waves, Bull.Seism. Soc. Amer. Vol.79, No.3, 1989, pp.610-630.

Kobayashi,S., Some Problems of the Boundary Integral Equation Method in Elastodynamics, Proc. 5th Int. Conf. on Boundary Elements, 1983, pp.775-784.

Mossessian, T.K. and Dravinski, M., Application of a Hybrid Method for Scattering of P, SV,and Rayleigh Waves by Near-surface irregularities: BSSA, 77,1987, pp.1784-1803.

Sanchez-Sesma ,F.J. and Esquivel,J.A., Ground Motions on Alluvial Valley under the Incident Plane Waves, Earthq. Eng. & Struct. Dyn., Vol.7, 1979, pp.441-450.

Sanchez-Sesma, F.J., Bravo, M.A. and Herrera, I., Surface Motion of Topographical Irregularities for Incident P,SV, and Rayleigh Waves, BSSA, 75, 1985, pp.263-269.

Shinozaki,Y. High Frequency Response of a Sediment-filled Valley for Incident Plane SH Waves, IAEE/IASPEI Joint Working Group on Effect of Surface Geology on Seismic Motion, 1988,V/1-20.

Takemiya, H. and Arioka, K., Numerical Computation Method of Green Functions 2D Viscoelastic Layered Halfspace for Buried Uniformly-distributed Loads, Proc. JSCE, (submitted).

Takemiya,H., Ono, M., Suda,K. and Sugano,Y., Hybrid Analysis f Topographical Site Response and Its Characteristics, Proc. Japs Earthquake Engineering Symposium, 1990.

Toki,K. and Sato,T., Seismic Response Analysis of Ground wi Irregular Profiles by the Boundary Element Method, Proc. 5th In Conf. Boundary Elements, 1983, pp.699-708.

Trifunac,M.D., Scattering of Plane SH Waves by a Semicylindric Canyon, Earthquake Eng. & Struc. Dyn., Vol.1, 1973, pp.267-281.

Vogt,R.F. Wolf,J.P. and Bachmann,H., Wave Scattering by a Canyc of Arbitrary Shape in a Layered Half-space, Earthq. Eng. and Struc Dyn., Vol.16, 1988, pp.803-812.

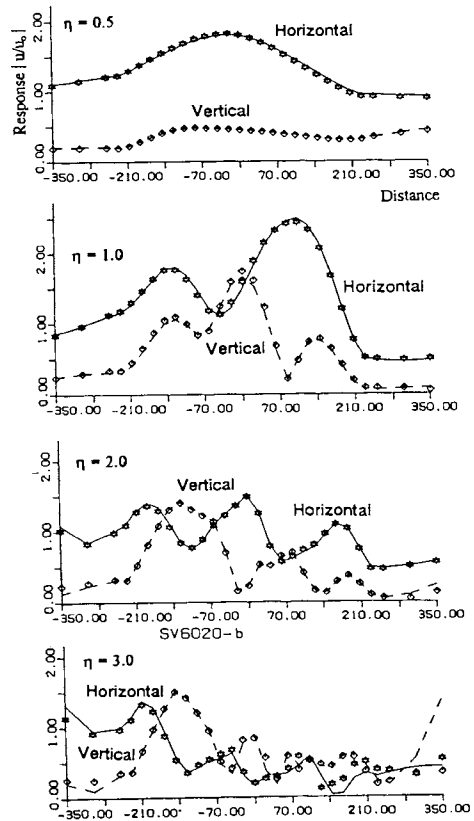
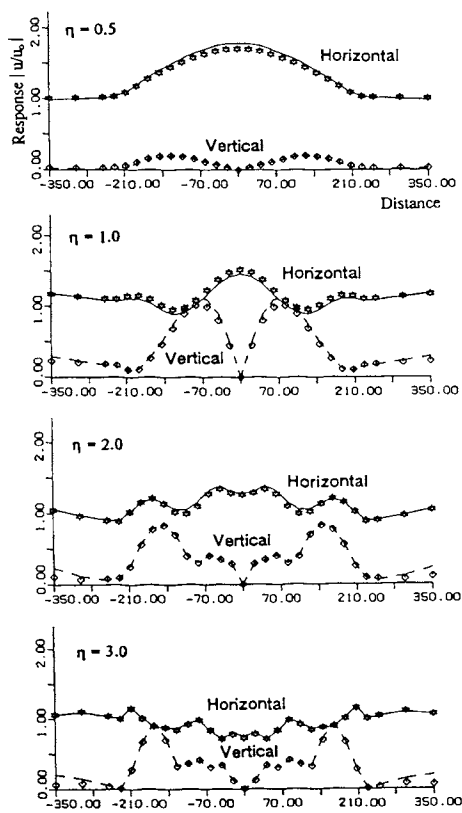
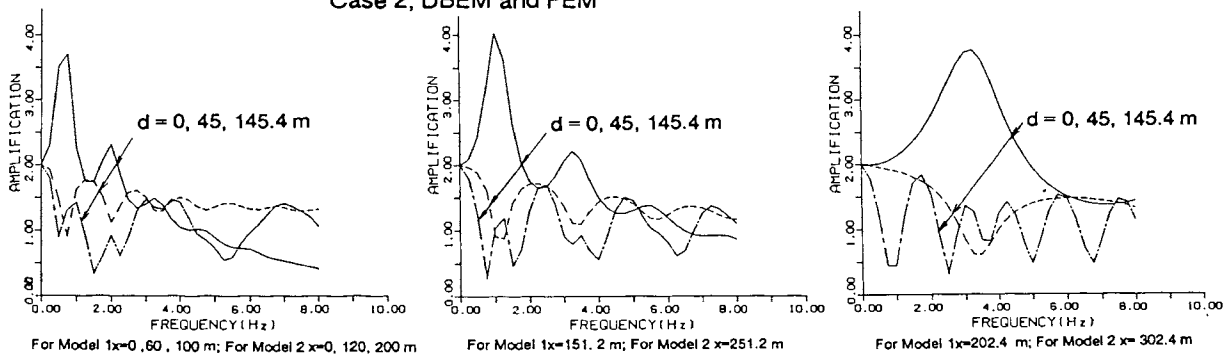
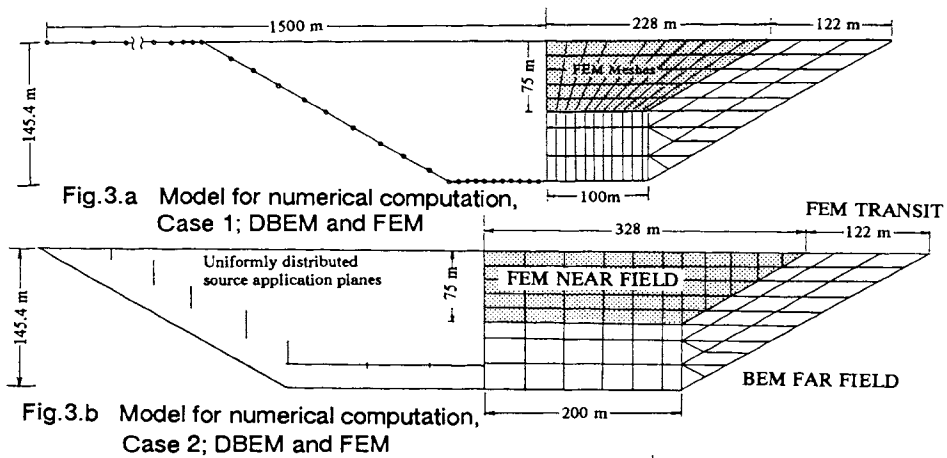
Wong,H.L. and Trifunac,M.D., Scattering of Plane SH Waves by Semi-Elliptical Canyon, Earthquake Eng. & Struc. Dyn., Vol.3, 1975, pp.157-169.

Wong,H.L. and Jennings,PC., Effect of Canyon Topography on Stron Ground Motion, Bull. Seism. Soc. Amer., Vol.65, No.5, 1975 pp.1239-1257.

Wong, H.L.: Effect of Surface Topography on The Diffraction of P,SV and Rayleigh Waves, BSSA, 1982, 72, pp.1167-1183.

Table 1 Soil Properties

	Shear velocity	Density	Damping	Poisson ratio
Alluvium Deposit	200 m/s	1.60 t/m <sup>3</sup>	0.10	0.45
Far Field	500 m/s	2.00 t/m <sup>3</sup>	0.02	0.35



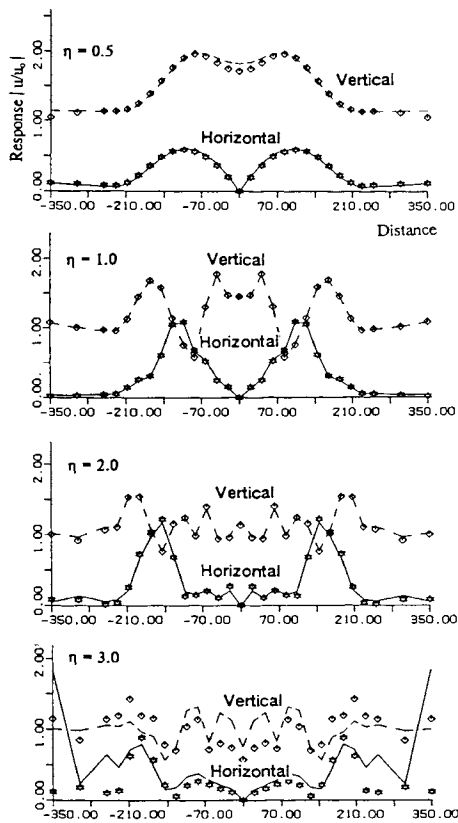


Fig.6.a Surface response,Case 1;  
P wave incidence, Angle of incidence  $\pi/2$

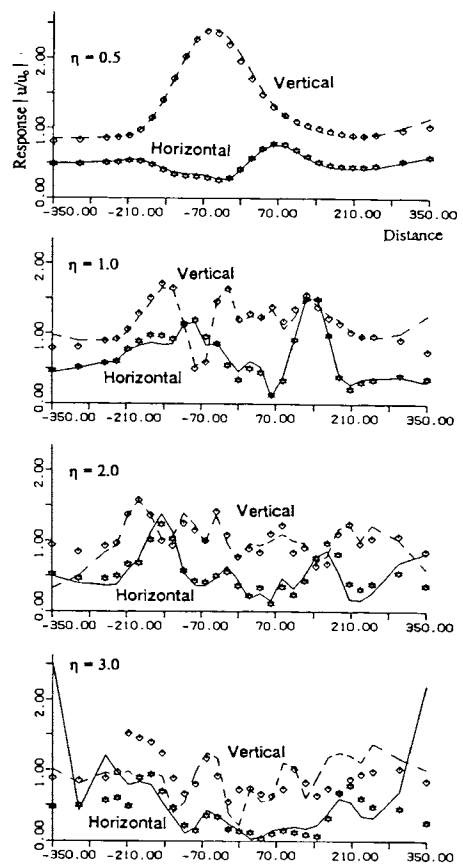


Fig.6.b Surface response,Case 1;  
P wave incidence, Angle of incidence  $\pi/3$

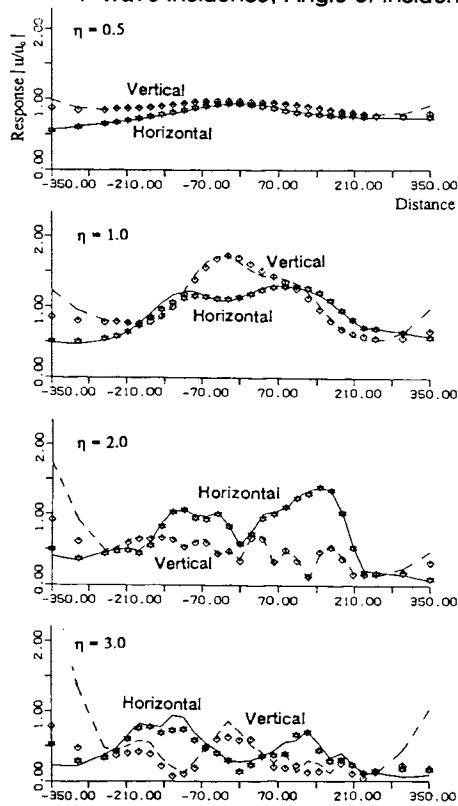


Fig.7 Surface response, Case 1;  
Rayleigh wave incidence

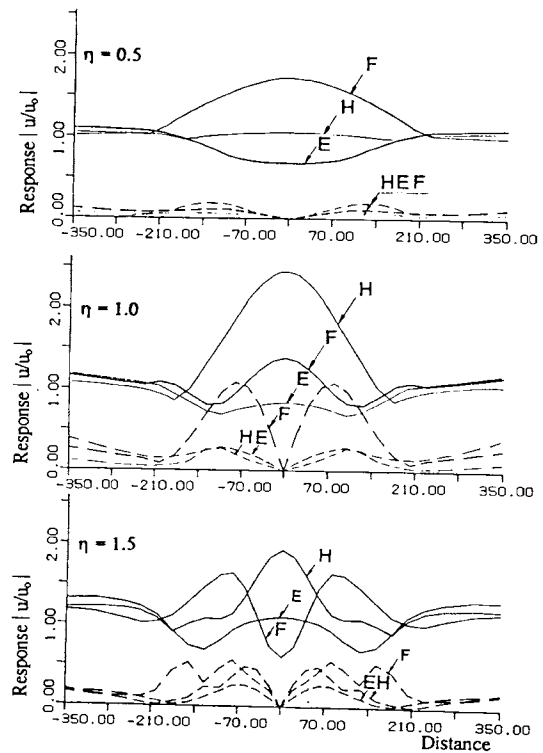


Fig.10 Subsurface topographical effect on surface response  
Case 1 F:  $D/H=1$  H:  $D/H=3/5$  E:  $D/H=0$

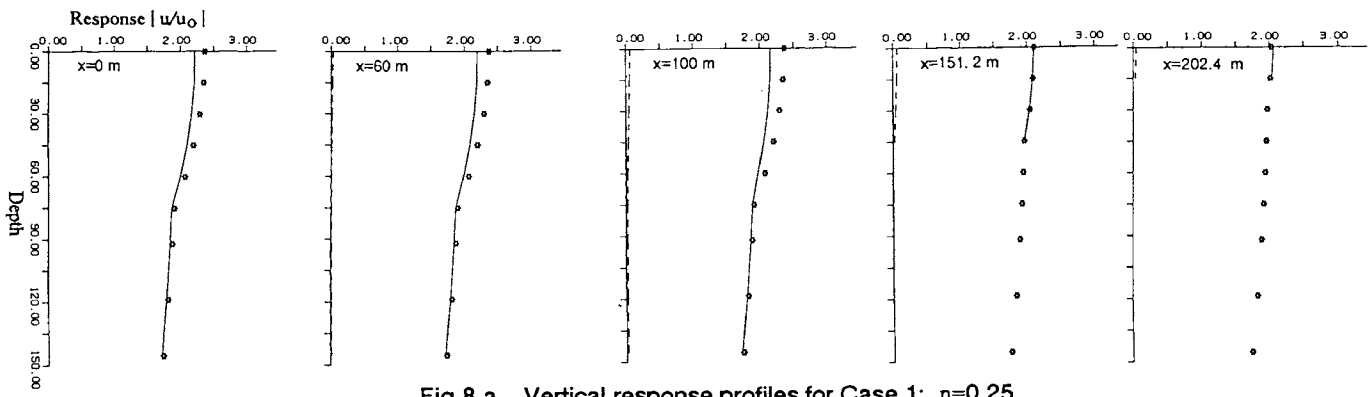


Fig.8.a Vertical response profiles for Case 1;  $\eta=0.25$

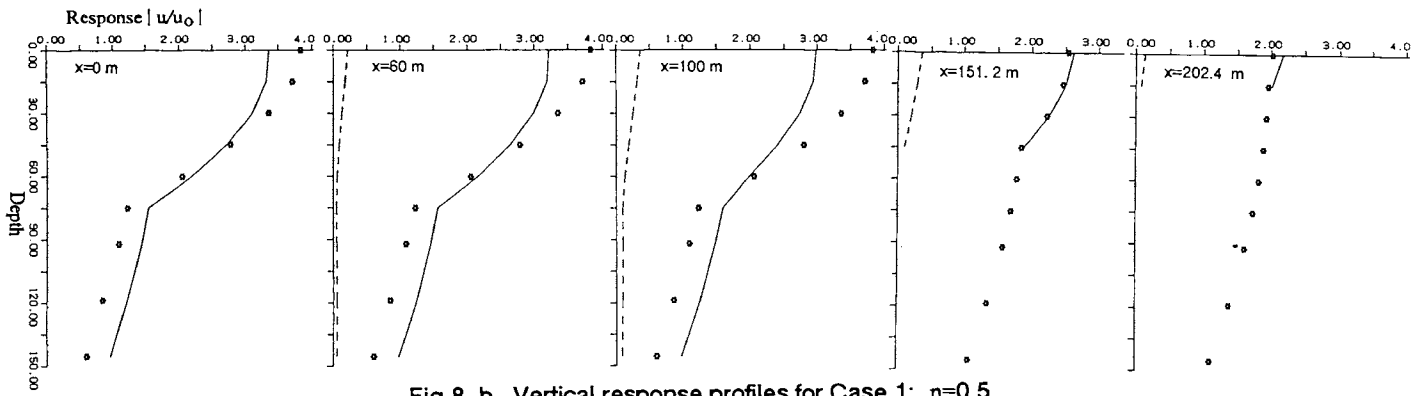


Fig.8.b Vertical response profiles for Case 1;  $\eta=0.5$

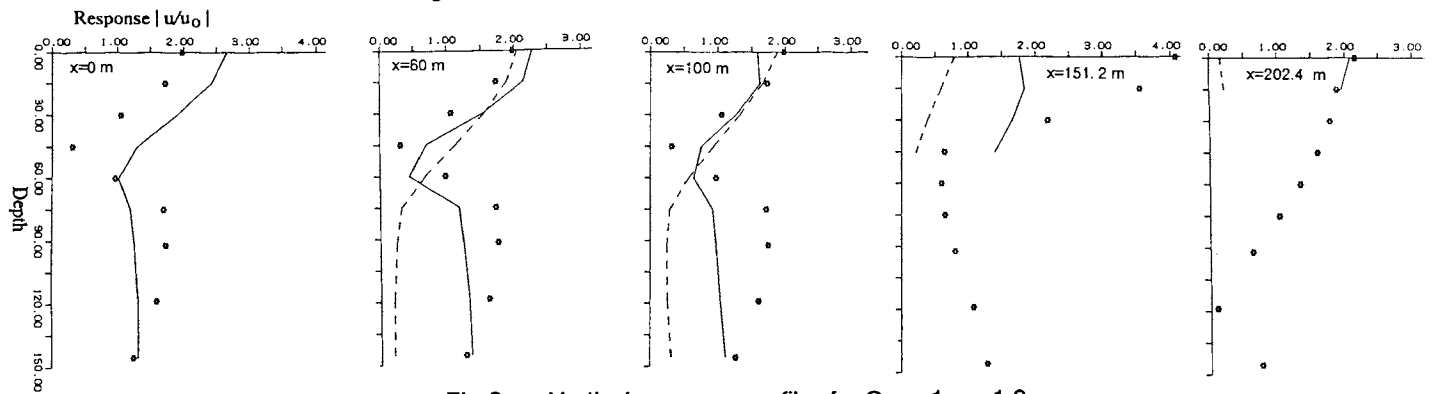


Fig.8.c Vertical response profiles for Case 1;  $\eta=1.0$

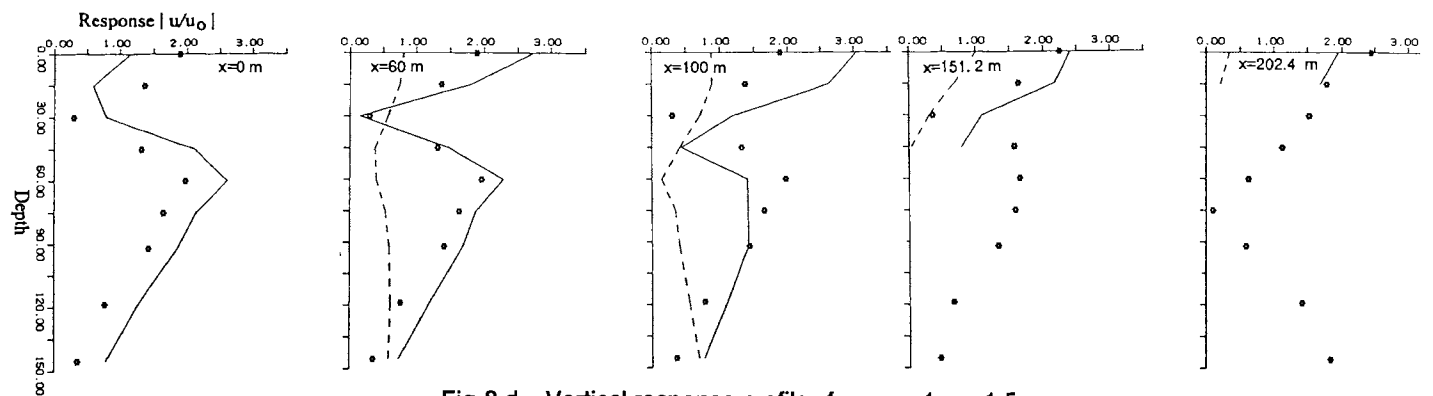


Fig.8.d Vertical response profiles for case 1;  $\eta=1.5$

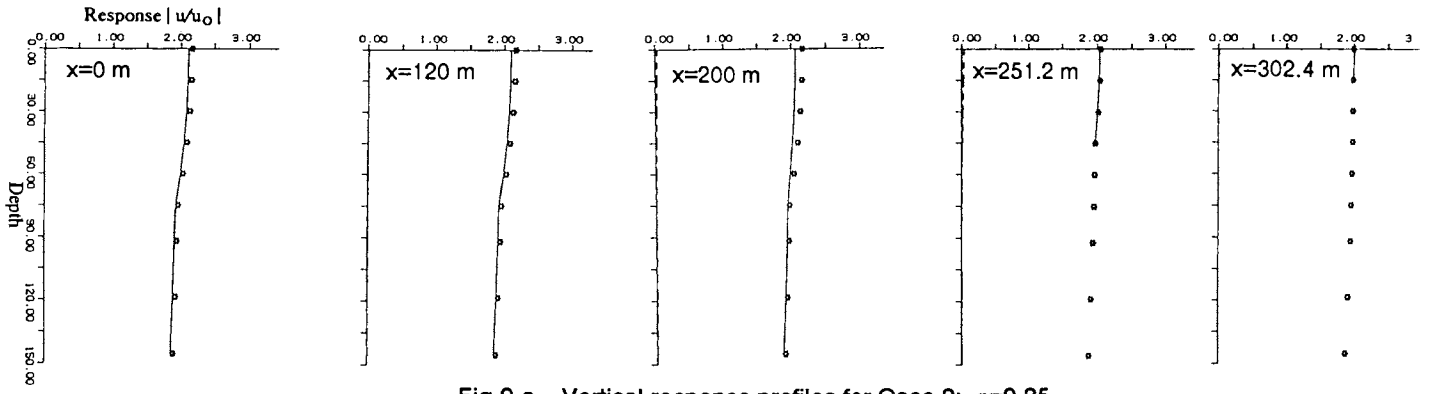


Fig.9.a Vertical response profiles for Case 2;  $\eta=0.25$

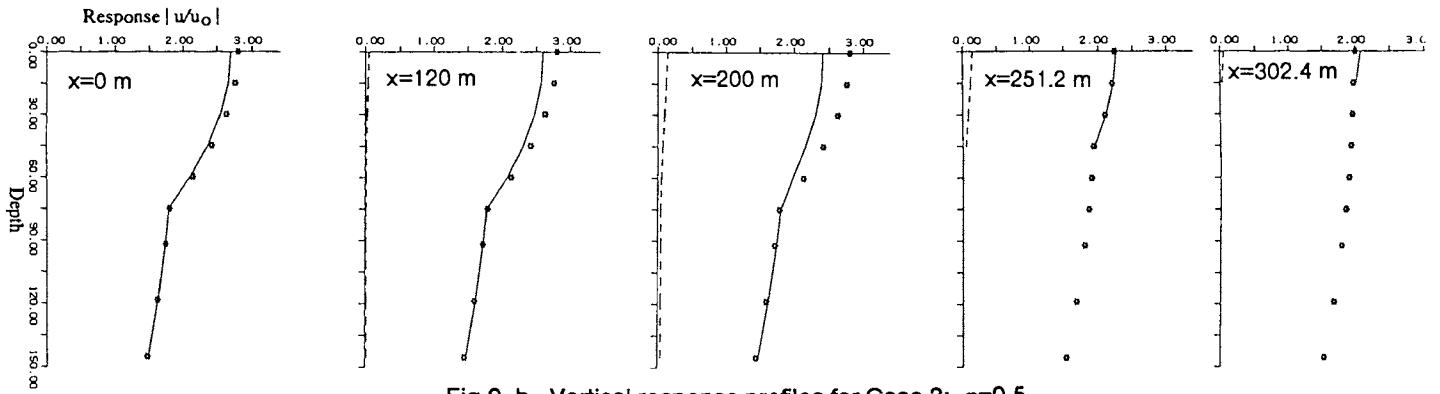


Fig.9.b Vertical response profiles for Case 2;  $\eta=0.5$

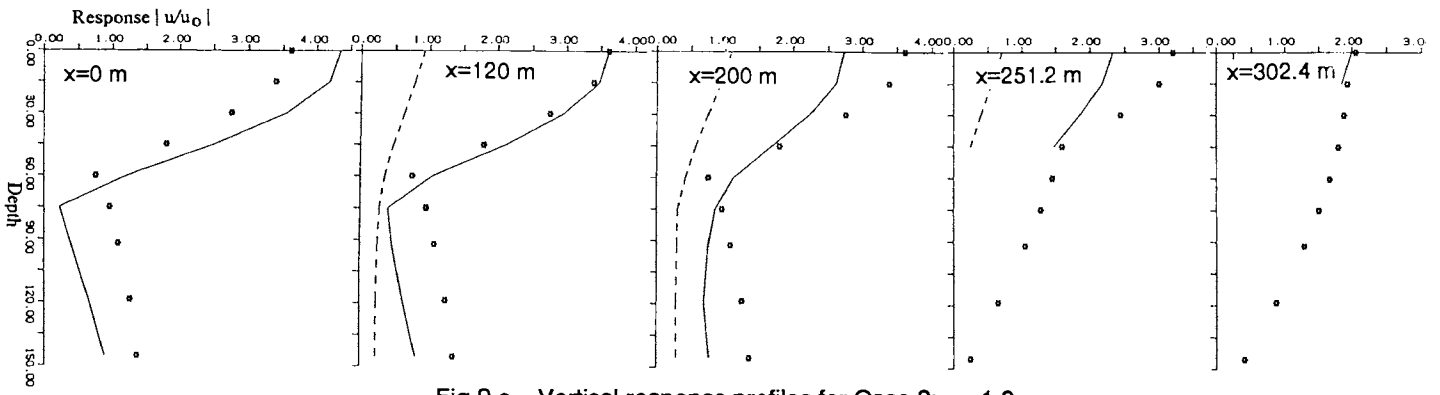


Fig.9.c Vertical response profiles for Case 2;  $\eta=1.0$

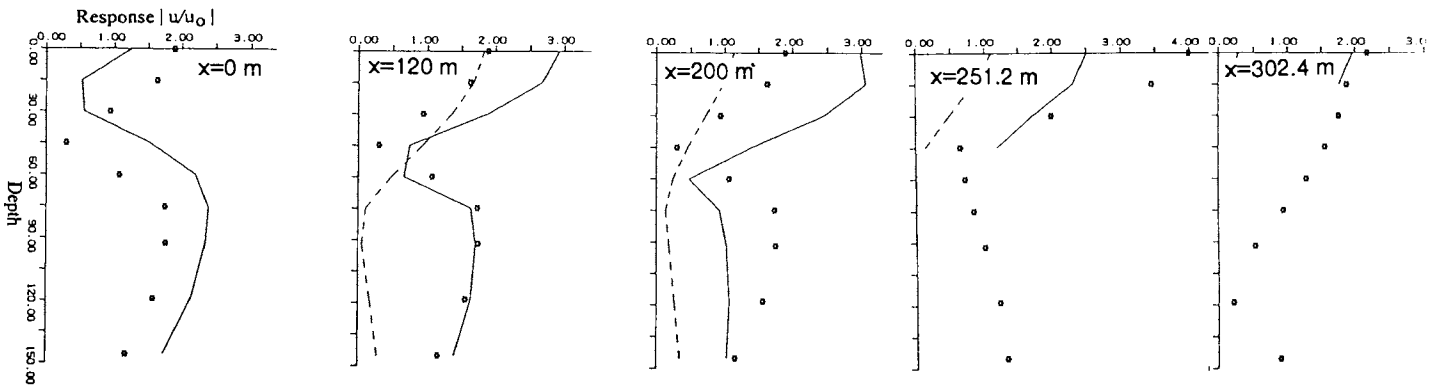


Fig.9.d Vertical response profiles for case 2;  $\eta=1.5$